6th International Conference
on
Wind Turbine Noise
Glasgow 20-23 April 2015

An Experimental and Numerical Parameter Study on Trailing Edge Blowing for Reduced Trailing Edge Noise

T. Gerhard University of Siegen, 57068 Siegen, Germany
E-Mail: tom.gerhard@uni-siegen.de

S. Erbslöh Senvion SE, 24783 Osterrönfeld, Germany
E-Mail: sascha.erbslöh@senvion.com

T. Carolus University of Siegen, 57068 Siegen, Germany
E-Mail: thomas.carolus@uni-siegen.de

Summary

The paper focuses on trailing edge blowing (TEB) as a mitigation technique of the trailing edge noise (TEN) from blades of modern wind turbines. A TEB configuration developed earlier by the authors is applied to a S834 and DU93W210 airfoil section. The airfoil sections were tested in the small aero-acoustic wind tunnel of the University of Siegen. Experimental hot wire anemometry was utilized as well as a numerical flow simulation (Large Eddy Simulations). The acoustic sources - in terms of turbulent boundary layer and surface pressure statistics - were determined without and with TEB. The effect of different blowing jet velocities at a wide range of angle of attacks was studied.

In general, without TEB the turbulent flow field statistics is similar for both airfoils, but the frequency range of the peak fluctuations is slightly different. The most favourable blowing velocity was found to be slightly below 50 % of the free stream velocity. For the S834, with this blowing rate, the trailing edge noise was reduced by up to 3 dB over a wide range of angle of attacks. The benefits of TEB were less pronounced for the DU93W210. Here the location of transition of the boundary layer is closer to the trailing edge, with the consequence that from the beginning the turbulent fluctuations encountering at the trailing edge are smaller. This explains why location and strength of TEB for trailing edge noise reduction must be designed such that it matches the details of the turbulent boundary layer in the airfoil's trailing edge region.

1. Introduction The unsteady flow field created in the turbulent boundary layer of an airfoil embedded in a quiet flow is responsible for the radiated noise at almost any flow condition. The noise emissions are associated with vortical disturbances encountering at the airfoil trailing edge (TE) inducing surface pressure fluctuations which are scattered at the TE and then converted into acoustic emissions. Generally, this aero-acoustically generated sound mechanism is called TE noise (TEN) and was detected to be the dominant noise source of an airfoil in spatially and temporally homogenous flow (see e.g. Roger and Moreau [1], Roger [2]). Regarding modern wind turbines, the interaction of the aerodynamically effective surfaces, i.e. the rotor blades, with the atmospheric shear layer generates TEN which is the main contributor to the overall noise emissions. This was proved e.g. by Devenport et al.

[3] who used a phased array technology to detect the TEN of three different wind turbine airfoils. Furthermore, Oerlemans et al. used microphone arrays to investigate the main self noise sources of six wind turbine airfoils in an aeroacoustic wind tunnel [4] and to determine the acoustic properties of a full scale turning wind turbine [5]. The studies found TEN to be the dominant contributor to the overall wind turbine noise emissions.

Future onshore wind turbines will continue to grow in size to reduce the cost of the produced energy. To improve acceptance and profitability at the same time they need to employ noise reduction technologies which are efficient or are purely passive, for example by exploiting the pumping effect of the rotor, don't hinder blade handling and require no additional maintenance schedules. With the rotor operating, unlikely aircraft, constantly in the lower atmosphere with rain, ice, dirt or erosion commonplace the aforementioned requirements pose a significant challenge.

The present study is dealing with a possible TEN mitigation technique which shall be defined as trailing edge blowing (TEB). Besides traditional low noise design rules for airfoils, e.g. thin TE's to avoid so called blunt TEN (see e.g. Blake and Gershfeld [6]), a modified TE geometry e.g. by serrations, slits or brushes can diminish the emitted noise by destructive interferences and destroying spanwise coherences (see e.g. Dassen [7] Finez et al. [8], Oerlemans et al. [9] or Herr [10]). Other approaches deal with modified TE material such as a porous TE (e.g. Chanaud [11], Geyer and Sarradj [12]). In contrast, TEB does not passively modify the surface impedance, but is affecting actively the primary reason of TEN, the turbulent boundary layer upstream of the TE. The development of the boundary layer can be affected by blowing clean air out of surface openings like slits or holes. However, the use of TEB for acoustical reasons is somewhat rare. Common applications of TEB are active flow control (AFC) concepts used to delay the separation point to higher angle of attacks (AOA) or circulation control applications which increase the sectional lift coefficient of an airfoil by adding high momentum air into the low-momentum boundary layer (see e.g. Johnston et al. [13], Tongchitpakdee et al. [14], Shires et al. [15]). One main acoustic application of TEB is the mitigation of the rotor-stator interaction (RSI) noise by filling the wake deficit downstream of the rotor resp. stator in a fan stage. Sutliff et al. [16, 17] showed that blowing air from the blade trailing edges of a turbofan rotor provided a significant tonal noise reduction and a broadband noise reduction of appr. 2-3 dB. A study carried out by Winkler et al. [18] found a broad band noise reduction for a tandem airfoil assembly of up to 8 dB. Kohlhaas et al. [19] completely eliminated the first harmonic of the blade passing frequency sound of a fan stage by optimizing the spanwise blowing profile. Nevertheless, for both studies the beneficial effect was constrained to lower frequency due to high frequency self-noise of the jet.

In a recent study, the authors of the present paper showed, that besides the mentioned turbofan noise applications, TEB has the potential to reduce the TEN emissions of an isolated airfoil [20]. The study compared an unmodified S834 airfoil to three different TEB airfoils equipped with a spanwise blowing slot located on the suction side at 75%, 82.5% resp. 90% of the airfoils chord length. The most favourable configuration with the slot located at 90% chord provided a TEN reduction of appr. 3 dB in the dominant TEN frequency range. However, the study was limited to one profile and one specific operating point. Furthermore, the jet velocity ratio was fixed to half of the free stream velocity.

Consequently, the current paper is focussing on the variation of (i) the baseline profile, (ii) the operational range and (iii) the blowing velocity. In addition to the previously investigated S834 profile, designed by Somers [21] for small horizontal axis wind turbines, one favourable TEB concept is transferred to a DU93W210 airfoil,

a wind turbine dedicated airfoil developed at the Delft University of Technology (see e.g. Timmer and van Rooij [22]). For the variation of the blowing velocity the ejected mass flow rate is varied. Additionally, the experimental set up allows a variation of the angle of attack and thus enables the investigation of the TEB effect at different airfoil operating points.

2. Methodology

2.1 Airfoil Sections and Test Rig Two different unmodified baseline airfoils are investigated, Somers S834 airfoil [21] and the DU93W210 airfoil [22]. These baseline airfoils are labeled as reference airfoils from now on. The airfoil sections have a chord length of c = 0.2 m and an aspect ratio of 1.33. They are mounted vertically between sideplates $0.5 \cdot c$ downstream of the nozzle exit of an open aeroacoustic wind tunnel. Although the AOA was varied, the standard operating point (SOP) was set to an effective AOA α_{eff} such that an infinite aspect ratio section of the airfoil would operate at its optimal lift to drag ratio for a chord based Reynolds number of $Re = 3.5 \cdot 10^6$. To compensate for open wind tunnel installation effects, a correction as derived by Brooks et al. [23] is applied, resulting in a geometric AOA α_{geom}. However, the available small aeroacoustic wind tunnel provides a maximum flow velocity corresponding to $Re = 3.5 \cdot 10^5$ only. To mimic the 10-times higher target Reynolds number the location of boundary layer transition on pressure side (PS) and suction side (SS) were controlled by a zigzag tape. The tripping locations were selected such that they correspond to the chordwise locations of natural transition at $Re = 3.5 \cdot 10^6$. The locations of natural transition were found via the airfoil performance prediction tool XFOIL [24]. XFOIL yields overall airfoil characteristics as a function of airfoil shape, AOA, Reynolds and Mach number in an undisturbed flow. It is based on a linear-vorticity 2nd order accurate panel method coupled with an integral boundary layer method and an e^n-type transition amplification formulation [25] and allows a prediction of the transition locations. The tripping positions of the S834 baseline airfoil are depicted exemplary with the main dimensions of the airfoil in figure 1 (left). All investigations were carried out at a Mach-number of M = 0.075. Table 1 summarizes the resulting AOA and tripping positions for both investigated airfoils at the SOP. Unless stated otherwise, the presented results in this report are evaluated for $\alpha = \alpha_{eff,SOP}$.

Table 1. Angle of attack and surface tripping positions for both investigated airfoils.

	$\alpha_{eff,SOP}$ [°]	$\alpha_{geom,SOP}$ [°]	$(x/c)_{Trip,SS}$ [-]	$(x/c)_{Trip,PS}$ [-]
S834	4.7	12.7	0.17	0.76
DU93W210	4.1	11.1	0.41	0.51

2.2 Trailing Edge Blowing Airfoils The TEB airfoils are equipped with a blowing slot located on the suction side of the airfoil at $(x/c)_{slot}$ = 0.9. From now on the TEB airfoils are labeled as TEB_{S834} for the S834 based TEB airfoil and TEB_{DU93} for the DU93W210 based TEB airfoil. The cross-sections of both TEB airfoils are depicted in figure 1 (right).

In contrast to many earlier TEB studies we are not confining ourselves to a momentumless wake. It is rather a question of identifying the acoustically optimal blowing rate. Furthermore, one has to keep in mind that the jet self noise increases with increasing blowing rates and may counteract the acoustic benefit (see e.g. [20]). Hence, the blowing rate is defined as

$$u_b = u_{jet} / u_\infty , \tag{1}$$

where the air jet velocity is u_{jet} and the freestream velocity u_∞, will be varied from values of u_b = 0…1. The geometry of the internal slot and the shape of the airfoil

contour downstream of the slot have been developed utilizing 2D steady-state, incompressible Reynolds-averaged Navier-Stokes (RANS) simulations with the airfoil being placed in an effectively unbounded and undisturbed flow. One design target was to enable the jet even for u_b < 1 to follow the airfoil contour by virtue of the Coandă-effect. The slot height h_s is 1% of the airfoils chord length for all investigated airfoils and constant in spanwise direction. The reference airfoil and the front part of the TEB airfoils is CNC-milled from one piece of aluminium, the rear parts of the TEB airfoils (x/c > 0.7) are manufactured using a rapid-prototyping technique. This enables the realisation of the different blowing slot geometries while keeping the complex internal air distributing tubing.

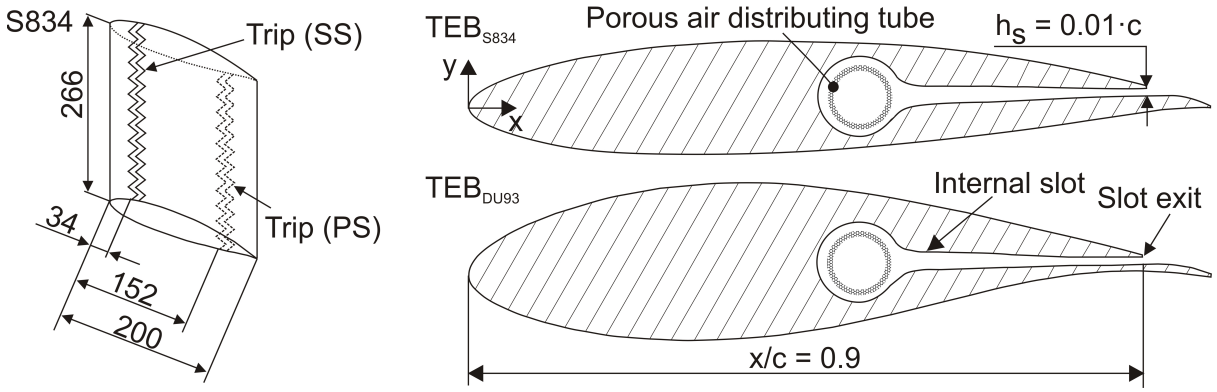

Figure 1. Left: Sketch of the S834 reference airfoil with trip positions (dimensions in mm, not to scale); right: Cross-sectional view of the TEB airfoils (not to scale).

2.3 Experimental Test Rig and Data Acquisition The ejected mass flow rate is controlled via a pneumatic circuit incorporating an external pressure source, a proportional pressure valve and a mass flow meter (ABB Sensyflow FMT200-ECO2), figure 2 (left). The pressurized air is fed into the airfoil section from both sides and distributed via a porous pressure tube towards the internal slot. Two external silencers attenuate extraneous noise emanating from the pressurized air supply system. Flow velocity and turbulence parameters in the airfoil boundary layer were measured with a 1-D hot-wire anemometer (HWA) (TSI™, type: 1210-T1.5), figure 2 (right). The probe is operating in a constant-temperature mode using the Streamline™ unit from Dantec Dynamics. For the exact positioning of the probe a three-axes traverse system was used.

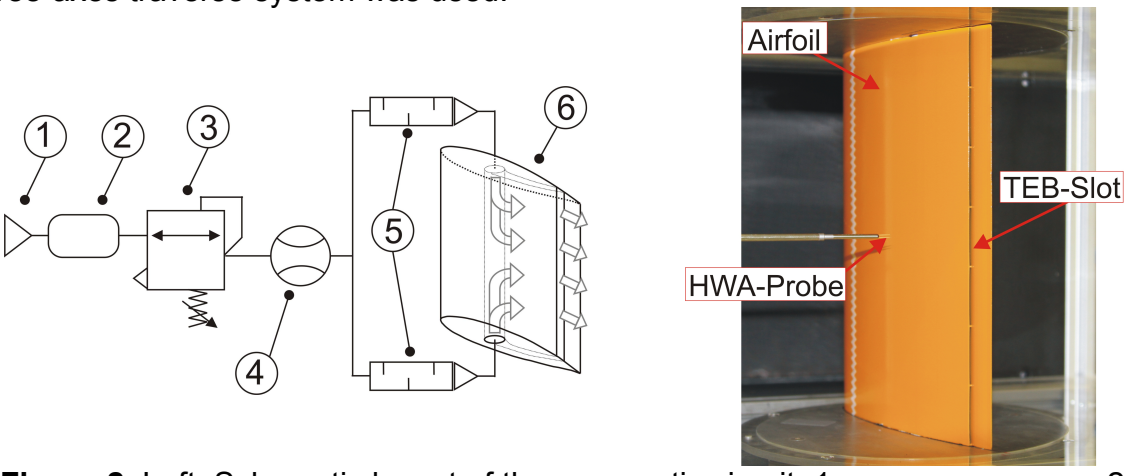

Figure 2. Left: Schematic layout of the pneumatic circuit: 1 - pressure source, 2 - compressed air reservoir, 3 - proportional pressure valve, 4 - mass flow meter, 5 - silencer, 6 - TEB airfoil; right: TEB$_{S834}$ airfoil and 1D HWA-probe (view from SS).

The wind tunnel (for details see Winkler and Carolus [21]) exhausts in a semi-anechoic chamber (4.5 m x 3.23 m x 2.9 m) which allows acoustic measurements according to ISO 3745 [26] down to 125 Hz. The characteristic turbulence intensity in a plane 0.01 m downstream of the wind tunnel nozzle exit is 0.2%. The sound from the airfoil sections was measured synchronously by two microphones (1/2" Brüel & Kjaer™, type 4190), located on pressure and suction side perpendicular to the TE and outside of the jet in a distance of 1.5·*c*. The microphones were equipped with a wind screen to avoid any flow induced pseudo sound, figure 3.

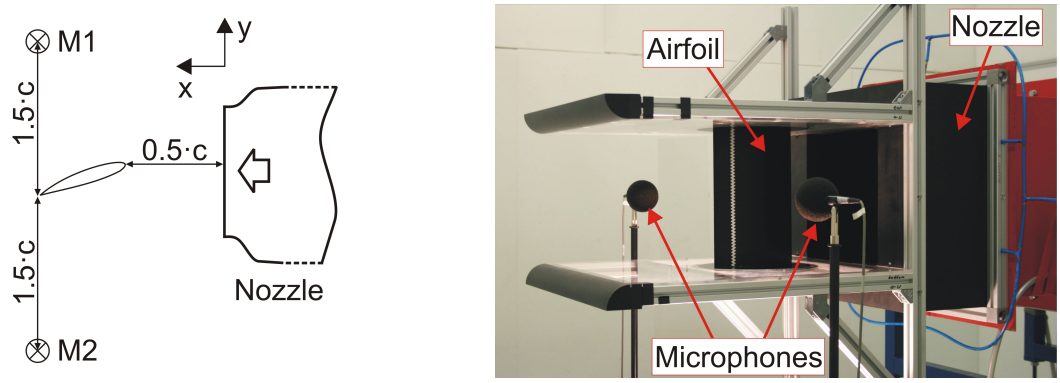

Figure 3. Left: Sketch of the airfoil section and the microphone positions (top view); right: Microphone arrangement around airfoil in the wind tunnel (view from PS).

2.4 Acoustic Signal Processing Techniques The determination of the acoustic signature of the airfoils was done by using different acoustic correlation techniques applied to the standard microphone configuration as well as to an advanced microphone array allowing the detection and quantification of TEN even at low signal-to-noise ratios (see Gerhard et al. [20, 27]). One correlation technique was found to reliably separate TEN from extraneous sound sources. The method takes advantage of the fact, that the overall airfoil self noise is dominated by the noise emissions occurring at the TE. Thus, the dipole characteristic of TEN offers the application of a correlation and filtering technique derived by Blake and Lynch [28]. The signals of the two TE phased-matched microphones (M1 and M2 in figure 3, left) should be equal in magnitude but 180° out of phase. The preparatory work is done by a 1st filter that removes all frequency components for which the level of the cross-spectral density (CSD) is less the 6 dB above the background CSD level. The 2nd filter rejects all frequencies where the phase shift of the CSD is not within a range of 180°±9°. Upon applying both filters, the spectrum contains theoretically pure TEN. The emitted free field sound pressure is then specified not as the sound pressure level of a single microphone but as the filtered CSD level of the two adjacent TE microphones L_{Spp}.

All unsteady quantities were captured with a sampling frequency f_s = 51.2 kHz. The spectral analysis is based on the power spectral density obtained by the *pwelch* routine in MATLAB® Vers. 2012a (Δf_{ref} = 1 Hz, $p_0 = 2 \cdot 10^{-5}$ Pa, f_0 = 1 Hz).

2.5 Numerical Set Up Transient numerical simulations allow a detailed view in the turbulent flow field around an airfoil, delivering e.g. the fluctuating surface pressure. However, transient simulations are very time consuming. Thus, the large eddy simulations (LES) carried out in this study are constrained to the SOP and, in terms of the TEB airfoils, to a blowing a rate of u_b = 0.5. The numerical domain covered 0.075·*c* of the airfoils spanwise extension and extended ~6·*c* in stream- and ~3·*c* in perpendicular direction, figure 4 (right). The boundary conditions of the LES computational domain were taken from a preceding fully turbulent RANS-simulation covering a domain that included the wind tunnel nozzle, the complete S834 reference

airfoil section with side plates and the anechoic chamber, in which the wind tunnel exhausts, figure 4 (left).

The RANS-predicted velocities were taken as boundary conditions at the inlet and side planes of the LES domain, in spanwise direction periodic boundary conditions were defined, the outlet was a pressure outlet. The 3D-block-structured numerical grid consists of $8.5 \cdot 10^6$ cells for the reference and appr. $11 \cdot 10^6$ cells for TEB airfoils, with an averaged local grid spacing of about $\Delta x^+ \approx 70$, $\Delta y^+ \approx 0.4$, $\Delta z^+ \approx 30$. The wall-resolving LES utilized a wall adaptive local eddy viscosity (WALE) subgrid-scale model by Nicoud and Ducros [29] and a dimensionless time step-size based on freestream velocity and chord length of $\Delta t = 6.4 \cdot 10^{-4}$. The convective Courant-Friedrichs-Lewy number exceeded only locally the value 1. The flow solver is based on a finite volume method and 2nd order accurate in space and time. For the time integration a bounded 2nd order implicit spatial scheme was used, the spatial integration was done by a bounded central differencing scheme. The achieved residuals of all variables are $1 \cdot 10^{-6}$. The simulations ran for appr. 15 flow-through times. The applied tripping was taken into account as an equivalent step with the height and an average length of the experimentally used zigzag tape, figure 5. The required mass flow rate for the jet of the TEB airfoils was considered in terms of a constant velocity boundary condition at the inlet of the internal slot. The commercial Navier-Stokes code ANSYS FLUENT™ version 14.5 has been used throughout this study. Table 1 summarizes the details of the experimentally and numerically cases investigated.

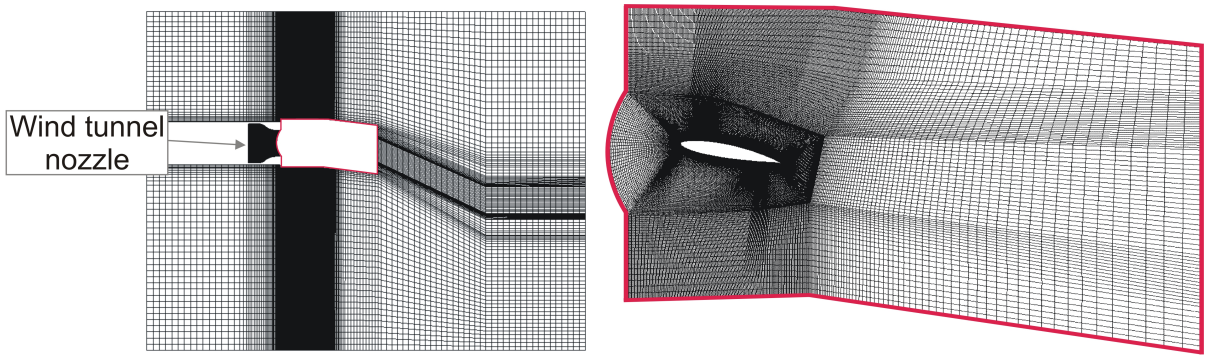

Figure 4. Left: Computational domain and grid topology for preceding RANS of complete set up; right: LES of the S834 reference; only every 2nd mesh line is drawn.

Figure 5. Numerical surface grid of the airfoil element; S834 reference (left) and TEB_{S834} (right).

Table 1. Operational range and blowing rates investigated.

Baseline airfoil	Airfoil configurations	Experiments		LES	
		α_{eff} [°]	u_b [-]	α_{eff} [°]	u_b [-]
S834	Reference	0...11	–	4.7	–
	TEB_{S834}		0...1		0.5
DU93W210	Reference	0...11	–	4.1	–
	TEB_{DU93}		0...1		0.5

3. Results

3.1 Flow field data Previous studies on the S834 airfoil [20] showed, that the TEB jet increases the velocity in the inner boundary where viscous shear dominates [30]. This increase causes an acoustically relevant decrease of the turbulence intensity, which is defined as the root-mean-square of the local velocity fluctuations normalized on the freestream velocity:

$$TI = u'_{rms}/u_{\infty}. \tag{2}$$

Figure 6 (left) shows a comparison of the experimentally determined and the LES-predicted velocity and turbulence intensity at x/c = 0.975 on the airfoil suction side of both investigated reference airfoils (y is perpendicular to the streamwise direction with y/c = 0 at the wall). The quantitative agreement is very satisfactory. Even though the *TI* is slightly underpredicted by the LES, all trends are depicted correctly. In the depicted SOP both airfoils show no TE stall. Note that the flow in the very near-wall region can not be resolved by hot wire anemometry because of the finite probe size.

Comparing the two reference airfoils, it becomes obvious, that the boundary layer of the S834 airfoil is thicker. Consequently, the *TI* increases earlier towards the wall and reaches a higher maximum. The LES predicts the maximum *TI* for the S834 at $y/c \approx 0.018$ and a decreasing *TI* below that point. In contrast, the *TI* in the boundary layer of the DU93W210 increases until y/c ≈ 0.003 where the slightly lower maximum value is reached. Hence, the overall maximum and the area of increased *TI* are larger for the S834 airfoil, but the DU93W210 shows the higher *TI* at the immediate wall.

An equivalent comparison of both reference airfoils to the TEB_{S834} resp. TEB_{DU93} is depicted in figure 6 (right). The LES predicted results show, that the displacement of the ejected mass flow postpones the upstream of the TEB slot developed boundary layer away from the wall and thus causes an increased boundary layer thickness for both airfoils. In spite of the identical blowing rate of both TEB airfoils (u_b = 0.5), the velocity in the jet core is above the predefined u_b. This difference can be attributed to the development of the blowing slot boundary layers reducing the effective slot exit area. Since the necessary mass flow rate is defined by the geometric slot area A_{slot}, the air density ρ and the desired blowing velocity u_{jet} as

$$\dot{m}_{blow} = \rho u_{jet} A_{slot}, \tag{3}$$

a reduced effective area leads to an increased jet velocity.

Additionally, the peak value of the jet core velocity, as well as the distance of the jet core to the wall varies for both TEB airfoils. This is due to the larger losses experienced by the jet of the TEB_{S834} airfoil which has to overcome a considerably larger momentum deficit than the jet merging into the boundary layer of the TEB_{DU93} airfoil. In terms of the TEB_{DU93}, the lower losses allow the jet to follow the airfoil contour more consequently and thus suppress the development of the new turbulent boundary layer between jet and wall.

Regarding the *TI*, the displacement of the jet causes that the peak *TI* of both TEB airfoils is postponed away from the wall. Simultaneously, the *TI* within the region of the jet core is reduced considerably. Here, for both TEB airfoils a reduction of up to 50% is predicted.

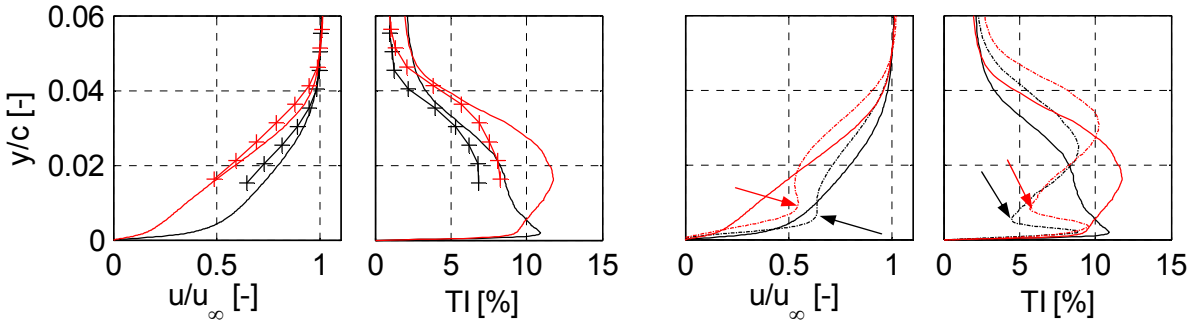

Figure 6. Velocity and *TI* distribution in the boundary layer (SS) at *x/c* = 0.975; left: LES and experimental results (reference airfoils, crosses indicate experiments); right: LES predicted results of reference and TEB airfoils (u_b = 0.5, dashed lines indicate TEB airfoils), the approximate core of the jet is indicated by an arrow; — S834, — DU93W210.

The level of the power spectral density (PSD) of the velocity fluctuations referenced to p_0 and plotted over 1/3-octave frequency bands is depicted for the S834 reference airfoil in figure 7 (a). The level increases towards the wall in the boundary layer. However, the peak level occurs around 500 Hz at some distance to the wall corresponding to the peak *TI* presented in figure 6 (*y/c* ≈ 0.015). Figure 7 (b) shows the difference of the PSD level of the DU93W210 and the S834 reference. Generally, the DU93W210 shows a lower level, especially the increase around 500 Hz vanishes. The slightly increased level close to the wall at higher frequencies (*f* > 1000 Hz) corresponds to the higher *TI* at the immediate wall (*y/c* < 0.01).

In figure 7 (c) and (d) the PSD level of the velocity fluctuations of the TEB airfoils are subtracted by their corresponding reference. Thus, negative values correspond to a decreased level due to the blowing jet. A general trend can be observed: The fluctuations at *y/c* > 0.02 are increased due to postponed boundary layer, below that point the TEB jet reduces the fluctuations. However, while the jet of the TEB_{DU93} is able to reduce the fluctuations completely in the immediate vicinity of the wall, the new boundary layer between jet and wall becomes obvious at *y/c* < 0.01 of the TEB_{S834}. Both TEB airfoils reduce the fluctuations up to 3 kHz.

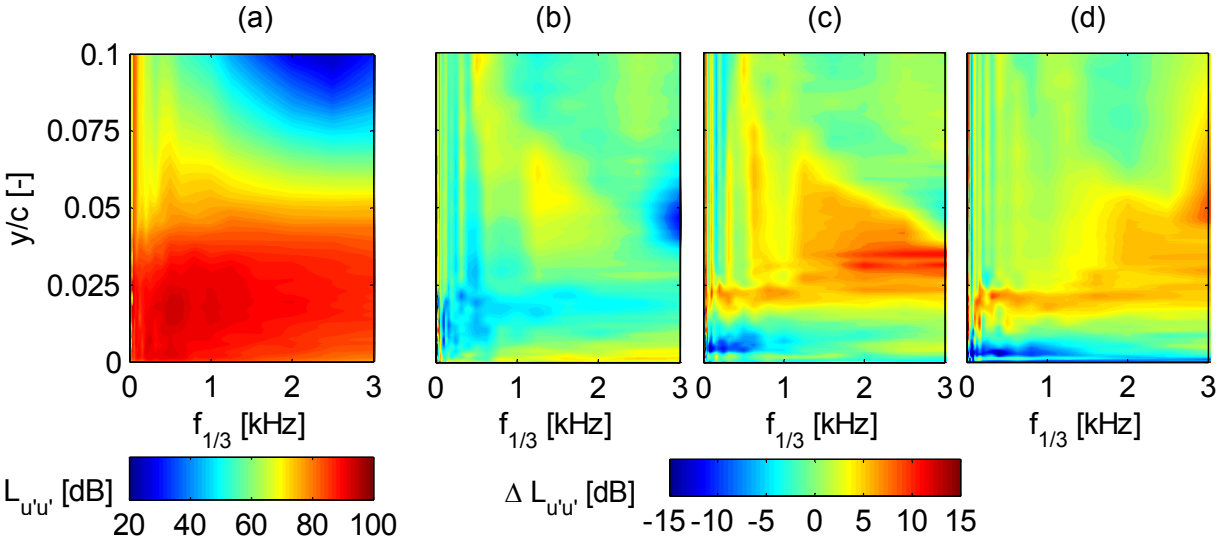

Figure 7. LES predicted PSD level of the velocity fluctuations (SS) at *x/c* = 0.975; (a) S834 reference airfoil; (b) Difference of S834 and DU93W210 reference; Difference of reference and TEB airfoil (u_b = 0.5): S834 (c) and DU93W210 (d).

A second, more relevant indicator for a possible acoustic effect of TEB are the induced surface pressure fluctuations beneath the turbulent boundary layer in the TE region. Figure 8 shows the LES predicted PSD level of the fluctuating pressure referenced to p_0 and plotted over the streamwise coordinate. For both reference airfoils (upper row) the level of the fluctuations increases towards the TE, but the frequency range of the peak fluctuations is somewhat different. While the spectral distribution at the TE of the S834 reference is dominated by lower frequencies, the dominant frequency region of the DU93W210 reference appears above 1000 Hz. This confirms the less intense velocity fluctuations in the DU93W210 boundary layer.

The effect of TEB (lower row) is again similar but not identical for both TEB airfoils. The blowing jet reduces the fluctuations predominantly in the lower frequency range by destroying larger turbulent structures developed in the original boundary layer upstream of the slot. Simultaneously, the jet itself consists of small scale turbulent structures contributing to higher frequencies. Due to the stronger turbulent structures present at lower frequencies for the S834 reference airfoil, the positive effect is more pronounced in terms of the TEB_{S834} for frequencies below 2 kHz. The same applies for the high frequency range (f > 3 kHz) where the pressure fluctuations of the S834 reference are less distinct, thus the increase is stronger. Note the logarithmic scale of the frequency axes in the diagrams.

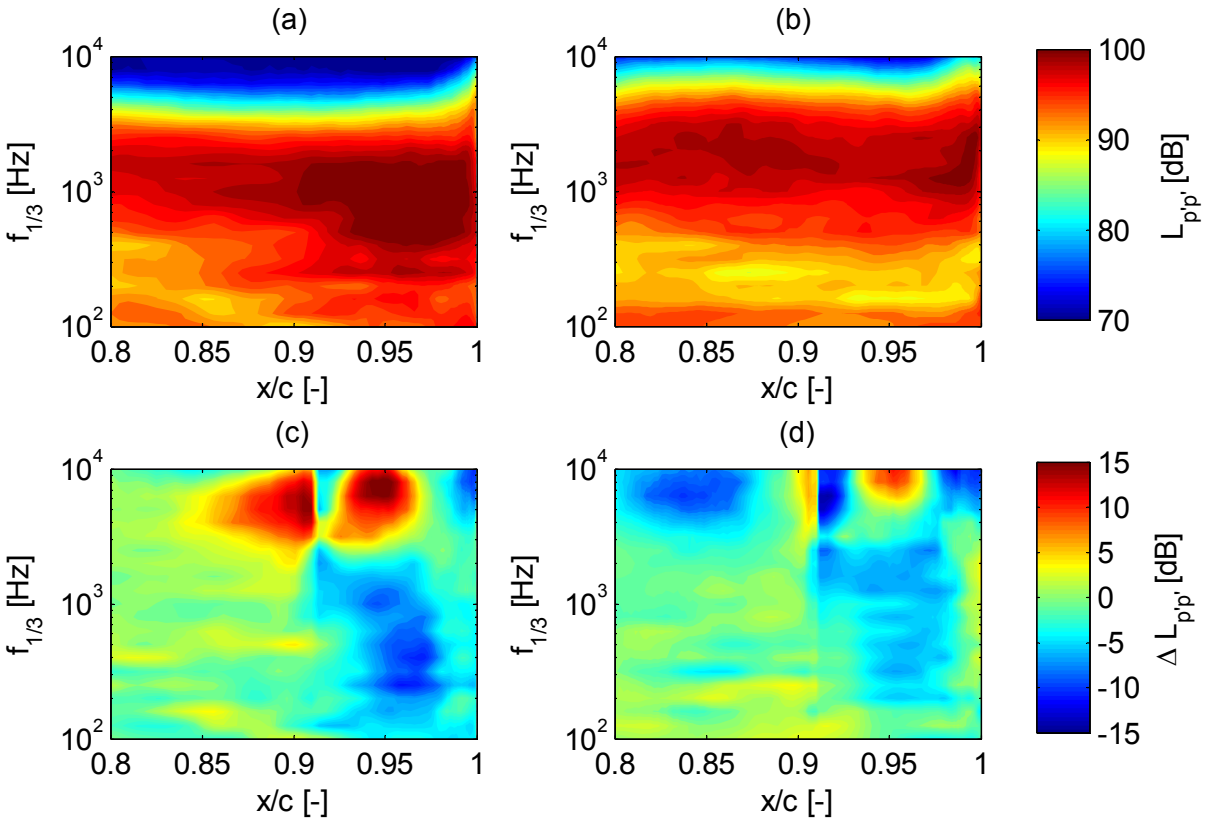

Figure 8. LES predicted PSD level of surface pressure fluctuations (SS); (a) S834 reference airfoil; (b) DU93W210 reference airfoil; Difference of TEB and reference airfoil (u_b = 0.5); S834 (c) and DU93W210 (d).

3.2 Acoustic results The acoustic evaluation and characterization of the airfoil self noise was shown in detail in a previous publication [27]. TEN was found to be the main airfoil self noise mechanism at frequencies from 160 Hz to al least 3 kHz with a spectral hump around 500 Hz dominating the spectrum. Above and below that frequency range the background noise of the wind tunnel drowns the airfoil noise. Figure 9 (left) shows the difference between the background noise (empty wind

tunnel) and both reference airfoils, here in terms of 1/3-octave frequency bands. Between 300 Hz and 1000 Hz the noise of both airfoils is significantly above the background noise level. Within that frequency range the level of the DU93W210 airfoil is appr. 1.5 dB below the S834 level. This proves the results of the flow-field data evaluation.

A narrow band spectrum of L_{Spp} ascertained with and without the airfoil sections present in the wind tunnel is depicted in figure 9 (right). The doubled filtered noise (data processing as described in section 2.4) shows TEN clearly between 300 Hz and 1500 Hz for both airfoils. At frequencies above 1500 Hz the signal-to-noise ratio is too low for a further identification of the DU93W210 TEN noise, up to 3 kHz only the TEN emissions of the S834 are detectable.

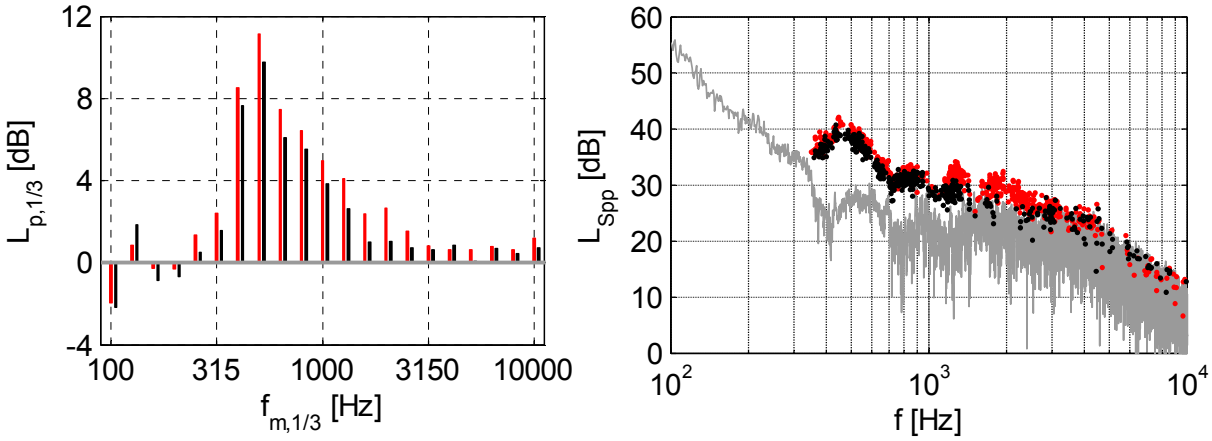

Figure 10. Left: 1/3-octave frequency bands of the measured sound pressure level of M2 referenced on the background noise; right: CSD level of M1 and M2; —/• S834 reference, —/• DU93W210 reference,— empty wind tunnel.

Figure 10 (upper row) shows the experimentally determined change of the sound pressure level due to TEB at the SOP. It becomes obvious, that the TEN emissions are considerably reduced only in case of the TEB_{S834}. The effect is constrained to the dominant TEN frequency range around 500 Hz, here a maximum reduction of appr. 3 dB is achieved for a blowing rate slightly below the so far discussed value of u_b = 0.5. The spectrogram of the DU93W210 is qualitatively similar, but the acoustic benefit is much less pronounced. At higher blowing rates the high frequency blowing self noise, i.e. the noise generated by the blowing jet, dominates the spectrum and thus prevents any acoustical benefit. These results confirm the flow field data evaluation showing a higher reduction potential due to TEB for the S834 airfoil. Note that below 300 Hz and above 3 kHz the airfoil noise is drowned by the background noise.

In the lower row of figure 10 the effect on the overall sound pressure level (*OASPL*) is shown as a function of u_b and α_{eff} (as stated earlier, all other results are evaluated for $\alpha_{eff,SOP}$). Due to the low signal to noise ratio at frequencies below 300 Hz and above 1000 Hz the *OASPL* is calculated only within this frequency range. The TEB_{S834} can reduce the *OASPL* over a wide range of angle of attacks with a maximum reduction of more than 3 dB around $\alpha_{eff} \approx 9°$. The preferable blowing rate providing the maximum reduction is independent from the AOA and slightly below u_b = 0.5. The TEB_{DU93} provides only small acoustic improvements towards higher AOA's. Additionally it becomes obvious, that TEB considerably reduces the noise emissions of the airfoils after stall occurs at an AOA of appr. $\alpha_{eff} \approx 8.5°$. Here, for both airfoils the noise emissions in the dominating TEN frequency range are reduced by up to 3 dB.

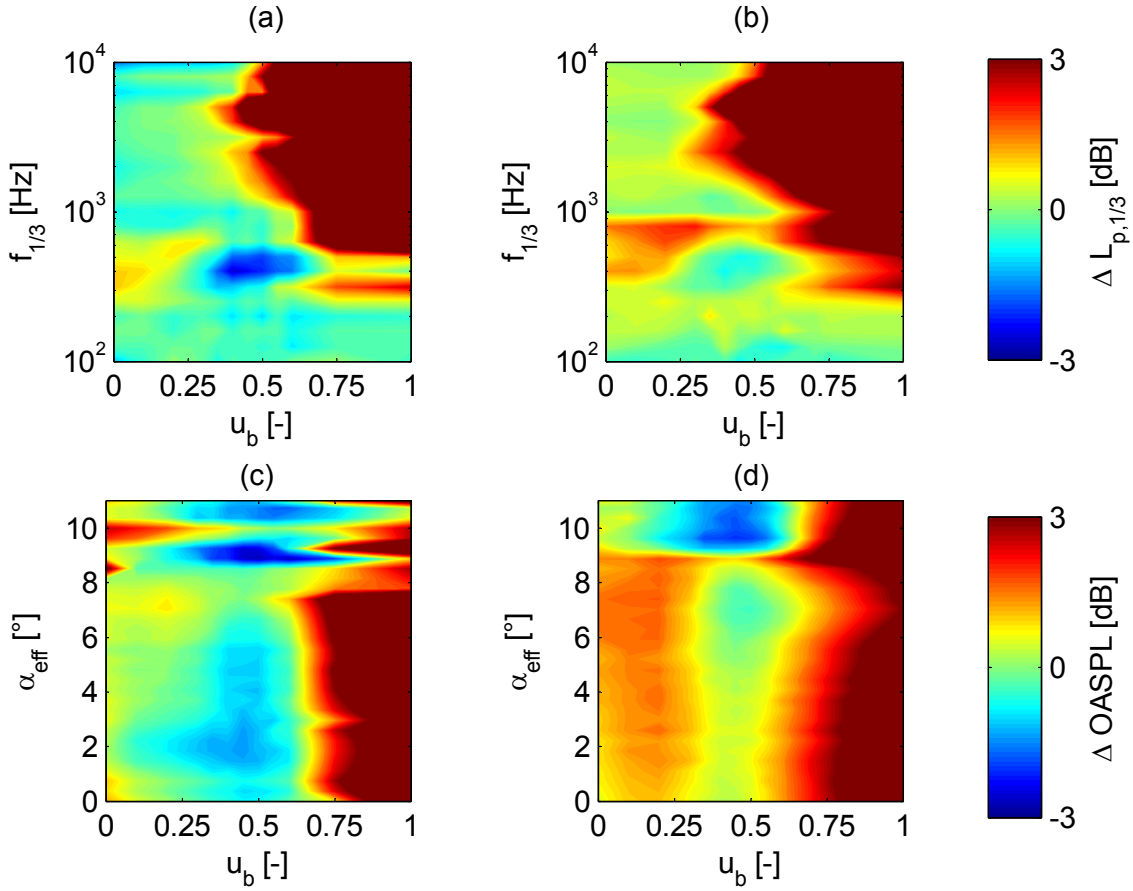

Figure 10. Difference of the TEB and the corresponding reference airfoil; upper row: $L_{p,1/3}$ ($\alpha_{eff} = \alpha_{SOP}$) for all measured u_b: (a) S834 and (b) DU93W210; lower row: OASPL calculated for 300 Hz < f < 1000 Hz: (c) S834 and (d) DU93W210.

4. Conclusions

Previous studies proved the trailing edge noise (TEN) reduction potential of the so called trailing edge blowing (TEB) applied to a stationary airfoil working at the optimal operating point. In the present study one promising TEB configuration was transferred from the originally investigated S834 airfoil shape to a DU93W210 airfoil. The effect of TEB was investigated experimentally and numerically for both configurations at varying blowing rates and at different angle of attack (AOA).

The evaluation of the flow field data showed, that the TEB jet reduces low frequency velocity fluctuations in the vicinity of the wall and thus the induced surface pressure fluctuations predominantly at lower frequencies (f < 1 kHz). At higher frequencies the jet itself increases the fluctuation level. This effect is similar for both airfoils, although the S834 shows a higher reduction potential due to more pronounced low frequent fluctuations in the TE region. The determination of the acoustic emissions shows quite similar results, the TEN can be reduced by up to 3 dB in the dominating frequency range below 1 kHz of the S834 spectrum. The most preferable blowing rate was found to be slightly below the intensively investigated blowing rate of u_b = 0.5. Furthermore the variation of the AOA showed that TEB can provide TEN reduction over a wide range of AOA's. Again the effect is similar for both investigated airfoils, however, corresponding to the flow field data evaluation, the total TEN reduction for the S834 is much more pronounced.

Generally, the TEN reduction potential of TEB depends on the airfoil characteristics in so far, that an early transition point leads to a more pronounced

turbulent boundary layer and thus causes more distinct TEN emissions. This is also proved by the noise reduction of both investigated airfoils after stall occurs. The TEB jet then protects the wall from the interaction with the large scale turbulent structures of the detached boundary layer.

The present study proves, that TEB can provide reduced TEN emissions at almost any airfoil shape as long as the TEB configuration is adapted to the respective airfoil. The slot should be positioned in the ultimate vicinity of the TE offering the opportunity of lower blowing rates to affect the ultimate TE region and to avoid blowing self noise emissions. A further variation and optimization of the blowing parameters in terms of the blowing geometry are subject of ongoing investigations. Another issue to be covered is the up-scaling to realistic Reynolds numbers of the results found so far. LES, large wind tunnel and/or full scale turbine tests will show how reliable the findings presented here are.

References

[1] MOREAU, S., ROGER, M., 2004, "Competing Broadband Noise Mechanisms in Low Speed Axial Fans", *Proc. of the 10th AIAA/CEAS Aeroacoustics Conference,* Manchester, UK, pp. 1-20.

[2] ROGER, M., 2006, "On the Noise from Open Rotors", *Proc. of the VKI Lecture Series 2006-05: Computational Aeroacoustics,* Rhode-St-Genèse, Belgium, pp. 1-18.

[3] DEVENPORT, W., BURDISSO, R. A., CAMARGO, H., CREDE, E., REMILLIEUX, M., RASNICK, M., VAN SEETERS, P., 2010, "Aeroacoustic Testing of Wind Turbine Airfoils", Subcontract Report for the National Renewable Energy Laboratory (Golden, Colorado), NREL/SR-500-43471, *Virginia Polytech Institute and State University*, Blacksburg, Virginia.

[4] OERLEMANS, S., 2004, "Wind Tunnel Aeroacoustic Tests of Six Airfoils for Use on Small Wind Turbines", Subcontract Report for the National Renewable Energy Laboratory (Colorado, USA), AAM-2-32237-01, *National Aerospace Laboratory NRL*, Emmeloord, Netherlands.

[5] OERLEMANS, S., SIJTSMA, P., MENDEZ LOPEZ, B., 2007, "Location and Quantification of Noise Sources on a Wind Turbine", *Journal of Sound and Vibration*, 299(4-5), pp. 869-883.

[6] BLAKE, W. K., GERSHFELD, J. L., 1989, "The Aeroacoustics of Trailing Edges", *Frontiers in Experimental Fluid Mechanics*, M. Gad-el-Hak, ed., Springer, Berlin, 46, pp. 457-532.

[7] DASSEN, T., PARCHEN, R., BRUGGEMAN, J., HAGG, F., 1996, "Results of a Wind Tunnel Study on the Reduction of Airfoil Self-Noise by the Application of Serrated Blade Trailing Edges", *1996 European Union Wind Energy Conference and Exhibition*, Gothenburg, Sweden.

[8] FINEZ, A., JONDEAU, E., ROGER, M., JACOB, M. C., 2010, "Broadband Noise Reduction With Trailing Edge Brushes", *16th AIAA/CEAS Aeroacoustic Conference*, Stockholm, Schweden.

[9] OERLEMANS, S., FISHER, M., MAEDER, T., KÖGLER, K., 2009, "Reduction of Wind Turbine Noise Using Optimized Airfoils and Trailing-Edge Serrations", *AIAA Journal*, 47(6), pp. 1470-1481.

[10] HERR, M., DOBRZYNSKI, W., 2005, "Experimental Investigations in Low-Noise Trailing-Edge Design", *AIAA Journal*, 43(6), pp. 1167-1175.

[11] CHANAUD, R. C., KONG, N., SITTERDING, R. B., 1976, "Experiments on Porous Blades as a Means of Reducing Fan Noise", *The Journal of the Acoustical Society of America*, 59(3), pp. 564-575.

[12] GEYER, T., SARRADJ, E., 2014, "Trailing Edge Noise of Partially Porous Airfoils", *20th AIAA/CEAS Aeroacoustic Conference*, Atlanta, GA.
[13] JOHNSTON, J. P., NISHI, M., 1990, "Vortex Generator Jets - Means for Flow Separation Control", *AIAA Journal*, 28(6), pp. 989-994.
[14] TONGCHITPAKDEE, C., BENJANIRAT, S., SANKAR, L. N., 2006, "Numerical Studies of the Effects of Active and Passive Circulation Enhancement Concepts on Wind Turbine Performance", *Journal of Solar Energy Engineering*, 128(4), pp. 432-444.
[15] SHIRES, A., KOURKOULIS, V., 2013, "Application of Circulation Controlled Blades for Vertical Axis Wind Turbines", *Energies*, 6, pp. 3744-3763.
[16] SUTLIFF, D. L., TWEEDT, D. L., FITE, E. B., ENVIA, E., 2002, "Low-Speed Fan Noise Reduction With Trailing Edge Blowing", *International Journal of Aeroacoustics*, 1, pp. 275-305.
[17] SUTLIFF, D. L., 2005, "Broadband Noise Reduction of a Low-Speed Fan Noise Using Trailing Edge Blowing", NASA/TM-2005-213814 and AIAA-2005-3028, *NASA Glenn Research Center*, Cleveland, Ohio.
[18] WINKLER, J., CAROLUS, T., SCHEUERLEIN, J., DINKELACKER, F., 2010, "Trailing-Edge Blowing on Tandem Airfoils: Aerodynamic and Aeroacoustic Implications", *Proc. of the 16th AIAA/CEAS Aeroacoustics Conference,* Stockholm, Sweden.
[19] KOHLHAAS, M., BAMBERGER, K., CAROLUS, T., 2013, "Acoustic Optimization of Rotor-Stator Interaction Noise by Trailing-Edge Blowing", *19th AIAA/CEAS Aeroacoustics Conference*, Berlin, Deutschland.
[20] GERHARD, T., ERBSLÖH, S., CAROLUS, T., 2014, "Reduction of Airfoil Trailing Edge Noise by Trailing Edge Blowing", *Journal of Physics: Conference Series*, 524(012123).
[21] SOMERS, D. M., 2005, "The S833, S834, and S835 Airfoils", Subcontractor Report NREL/SR-500-36340 for the Nationale Renewable Energy Laboratory (Golden, Colorado), NREL/SR-500-36340, *Airfoils Incorporated*, Port Matilda, Pennsylvania.
[22] TIMMER, W. A., VAN ROOIJ, R. P. J. O. M., 2003, "Summary of the Delft University Wind Turbine Dedicated Airfoils", *41st Aerospace Sciences Meeting and Exhibit*, Reno, Nevada.
[23] BROOKS, T. F., MARCOLINI, M. A., POPE, D. S., 1984, "Airfoil Trailing Edge Flow Measurements and Comparison with Theory Incorporating Open Wind Tunnel Corrections", *Proc. of the AIAA/NASA 9th Aeroacoustics Conference,* Williamsburg, Virginia, pp. 1-12.
[24] DRELA, M., 1989, "XFOIL: An Analysis and Design System for Low Reynolds Number Airfoils", *Low Reynolds Number Aerodynamics*, T. J. Mueller, ed., Springer, Berlin, Proceedings of the Conference Notre Dame, Indiana, USA, 5-7 June 1989, pp. 1-12.
[25] MUELLER, T. J., 2001, Fixed and Flapping Wing Aerodynamics for Micro Air Vehicle Applications, *American Institute of Aeronautics and Astronautics*
[26] ISO: INTERNATIONAL ORGANIZATION FOR STANDARDIZATION, 2003, "Determination of Sound Power Levels of Noise Sources Using Sound Pressure—Precision Methods for Anechoic and Hemi-Anechoic Rooms", ISO 3745: 2003.
[27] GERHARD, T., CAROLUS, T., 2014, "Investigation of Airfoil Trailing Edge Noise with Advanced Experimental and Numerical Methods", *21st International Congress on Sound and Vibration*, Peking, China.
[28] BLAKE, W. K., LYNCH, D. A., 2002, "Source Characterization by Correlation Techniques", *Aeroacoustic Measurements*, T. J. Mueller, ed., Springer, Berlin, pp. 218-257.
[29] NICOUD, F., DUCROS, F., 1999, "Subgrid-Scale Stress Modelling Based on the Square of the Velocity Gradient Tensor", *Flow, Turbulence and Combustion*, 62(3), pp. 183-200.
[30] SCHLICHTING, H., 1979, Boundary-Layer Theory, *McGraw-Hill, Inc.*